Annual Summary Document
Year: 2021
Months: 01.01.2021 – 31.12.2021

Project Title: Plasma harmonics for diagnosing plasma and driving laser

Project Work Plan (according to the contract)

Stage: II. Numerical simulations and experiments on HHG and generating-plasma dynamics

Activities:

II.1 Numerical simulations on HHG and plasma dynamics

II.2 Experiments on efficiency of HHG on solid and gas targets

II.3 Project management

1. Cover Page

Project title: Plasma harmonics for diagnosing plasma and driving laser
Project code: E_13/16.10.2020
Acronym: PHARDIPLAS

- **Group list (physicists, staff, postdocs, students);**

Physicist
Director of project: **Conf.dr. Mihai STAFE**
Team members:
Prof. dr. Niculae N. PUȘCAȘ
Ș.l.dr. Georgiana VASILE
Ș.l.dr. Constantin NEGUȚU

PhD students:
Alexandru ENCIU
Alexandru-Ferencz FILIP
Răzvan MIHALCEA

Staff: Ec. Ana-Maria Nicoleta DRAGOMIR

- Specific scientific focus of group (state physics of subfield of focus and group's role);

The scientific focus of the group was related to the numerical simulation (in COMSOL and MATLAB) of the harmonic generation process in the interaction of an intense laser pulse with a plasma. Validation of the theoretical model that we proposed and of the numerical results was another important task which was realized by carrying experiments in similar conditions with those from the simulations.

- Summary of accomplishments during the reporting period.

In Phase 2 we mainly realized the following objectives:

- developed a new theoretical „three step model" for harmonic generation in gas plasma

- developed scripts in COMSOL and MATLAB for 2D calculation of the properties of the harmonics (third, fifth, etc) generated in gas plasmas as a function of pump laser properties.

- developed script in MATLAB to evaluate numerically the momentum transferred by high power laser on solid targets in single and multi-pulse regime in connection to the plasma produced at the target surface.

- analyzed experimentally the properties of third harmonic radiation (i.e. intensity, time and space distribution) as a function of pump-laser properties: intensity, polarization

- published one Q2 paper on harmonics generation in an American journal:

M. Stafe, "Three-step model for third-harmonic generation in air by nanosecond lasers", JOURNAL OF THE OPTICAL SOCIETY OF AMERICA B-OPTICAL PHYSICS38 (7), 2206-2214 (2021)

- two papers in preparation: on non-linear optical effects induced by intense laser pulses, and on laser acceleration of solid targets and particles (in collaboration with INFLPR).

2. Scientific accomplishments – Results obtained during the reporting period.

Activity II.1: Numerical simulations on HHG and plasma dynamics

In the last years several authors investigated extensively the phase matching limitations associated with focal geometry in the process of harmonics generation.Typically, a particular generated harmonic and the fundamental laser field are matched in phase over distances that are many times the wavelength of the incident light. However, the length over which the harmonic phases are matched (i.e. the coherence length) can be much shorter than the focal depth (typically, 1 mm) owing to different rates of diffraction for different wavelengths. Because of these issues, it is typical to confine the interaction region in the non-linear (NL) medium to a single geometrical coherence length to avoid destructive phase cancellations. This is usually done by lengthening the laser focus relative to the width of the NL medium by working outside of the focus. As mentioned above, this method does not utilize the high-intensity focal volume outside of the coherence length. After a coherence length, new harmonic production is out of phase with previously generated harmonic light (Fig. 1) The generation of a particular harmonic can go in and out of phase many times in the laser focus. Harmonic light generated at the first

position is out of phase with the harmonic light generated at the second position, but in phase with the light generated at the third position.

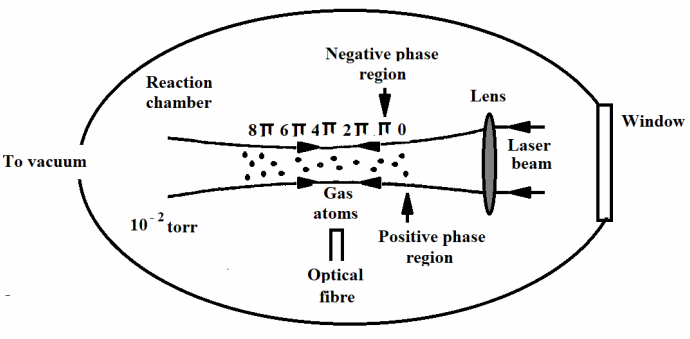

Fig. 1. Phase variation of harmonic emission throughout the laser focus.

Numerical simulation of harmonics generation with COMSOL/MATLAB

The generation of third, fifth, … *q*-th harmonic in a homogenous gas plasma is described by the NL polarization oscillating at q-th frequency:

$$P_{NL\,y}(\omega_q = q\omega) = \varepsilon_0 \chi^{(q)} \left(E_{\omega y}\right)^q . \quad (1)$$

The coupled wave equations describing the propagation of the fundamental (F, q=1) and third harmonic (TH, q=3) radiations within the NL medium can be written vectorially in a concise way as follows:

$$\nabla \times (\nabla \times E_q) - k_q^2 \left(\varepsilon_{rq} - \frac{i\sigma_q}{\omega_q \varepsilon_0}\right) E_q = \omega_q^2 \mu_0 P_{NL}(\omega_q) \quad (2)$$

Here, ε_{rq} denotes the frequency dependent dielectric constant of the NL medium due to neutral molecules, describing the positive dispersion of the medium: ε_{r1} = 1.00055 and ε_{r3} = 1.00057. σ_q is the frequency dependent plasma conductivity, the imaginary part of σ_q describing the anomalous negative dispersion. σ_q is directly related to the free electron density, and thereby to the nitrogen ions density N_i. The third order susceptibility $\chi^{(3)}$ is also directly related to the density N_i.

We used Newton method implemented in COMSOL software to solve numerically the coupled Eqs. (2) in the frequency domain. For time-dependent case, we use an accurate time-dependent solver with implicit time stepping method: generalized alpha method which contains a parameter, called alpha in the literature, to control the degree of damping of high frequencies. The output data of the COMSOL are stored in Excel worksheets. These worksheets act both as data storage and as feed-in for a successive program in MATLAB that processes these data to calculate additional characteristic measures of the non-linear process.

Due to the symmetry of the problem, we chose a 2D rectangular domain with the *x* axis corresponding to the propagation direction of the radiation, and *y* to the polarization direction. The origin of the *x* axis is in the focal plane and the origin of *y* axis is in the center of the F gaussian beam. The dimensions of the rectangular domain are $4x_0$ in the axial *x* direction and $8w_0$ in the transverse *y* direction. Here, x_0 is the Rayleigh length and w_0 denotes the beam waist. In 2D geometry, the Gaussian profile of the F pulse impinging on the front boundary positioned at $x = -2x_0$ is defined as

$$E_{1y,inc} = E_0 \sqrt{\frac{w_0}{w}} \exp\left(-\frac{w^2}{2w_0^2}\right) \exp\left[-i\left(k_1 x + k_1 \frac{y^2}{R} - \eta\right)\right], \quad (3)$$

whereas there is no incident field at TH frequency on the front boundary: $E_{3y,inc} = 0$. Here, E_0 is the field amplitude, $w(x)$ denotes the beam radius at axial *x* position, $R(x)$ is the position dependent wavefront radius, and $\eta(x) = 0.5\ \mathrm{atan}\left(\frac{x}{x_0}\right)$ is the Gouy phase shift of the Gaussian beam near its waist.

The boundary conditions for the wave Eqs. (2) are set as follows. The front boundary condition is set to "scattering boundary", with incident field given by Eq. (3):

$$e_n \times (\nabla \times E_q) - ik_q e_n \times (E_q \times e_n) = -e_n \times \left(E_{q,inc} \times \left(ik_q (e_n - e_k)\right)\right) \exp\left[\left(-ik_q r\right]\right) \quad (4)$$

Here, e_n is the unit vector normal to the boundary surface, and e_k is the unit vector giving the incident wavevector direction. The back boundary condition, positioned at $x = 2x_0$, is also set to "scattering boundary", with no incident field:

$$e_n \times (\nabla \times E_q) - ik_q e_n \times (E_q \times e_n) = 0 \quad . \quad (5)$$

The lateral boundaries, positioned at $y = 0$ and $y = 8w_0$, are set to "perfect electric conductor":

$$e_n \times E_q = 0 \quad . \quad (6)$$

The 2D spatial mesh is set linear in both *x* and *y* directions, with a minimum step of 30 nm. Fig. 2 presents numerical results regarding the influence of pump-laser intensity, NL medium length, and focus position in the NL medium. Fig 2(a) indicates that intensity of TH radiation increases approximately linearly with third power of the pump intensity. Fig 2(b) indicate a maximum signal when the NL medium length *L* is equal to confocal parameter *b* (b=2x_0), followed by a decrease of the efficiency as the length of the NL medium increases.

Fig 2(c) indicates that the focus position is also an important factor in determining the TH signal: focusing the pump laser behind the NL medium leads to stronger signal as compared to focusing in center or in front of the NL medium.

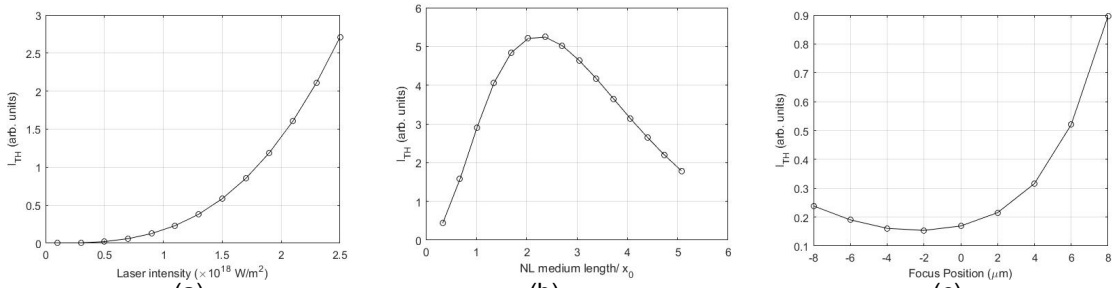

Fig. 2. Influence of different parameters on the intensity of third harmonic radiation: (a) pump intensity, (b) length of the NL medium, and (c) focus position in the NL medium.

We also modeled the harmonics generation by using ultrashort fs pulses. In this case, the non-linear time dependent wave equation is:

$$\nabla \times \left(\nabla \times \vec{E}\right) + \mu\sigma \frac{\partial \vec{E}}{\partial t} + \mu \frac{\partial}{\partial t}\left(\varepsilon_0 \frac{\partial \vec{E}}{\partial t} - \vec{P}\right) = 0 \quad (7)$$

where $\vec{P}$ has linear and nonlinear parts. The Fourier transform of the distorted output field field reveals the third harmonic radiation (Fig. 3). Comparing Figs 3(a) and 3(b), one can see that TH radiation is generated more efficiently for L=2x_0 as compared to L=4x_0, due to the value of the coherence length. These results are also consistent with the data presented in Fig. 2(b).

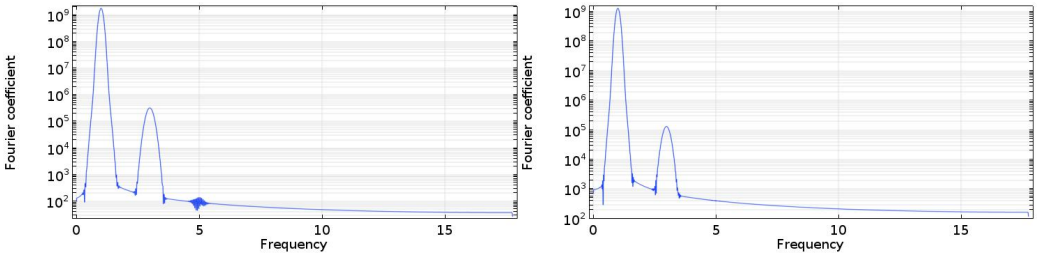

Fig. 3. Fourier transform of the time dependent output signal demonstrates the presence of third harmonic signal along with the pump signal. The simulations were carried for two lengths of the NL medium: (a) $L=2x_0$, (b) $L=4x_0$.

Activity II.2: Experiments on efficiency of HHG on solid and gas targets

Experiments on generation and characterization of TH radiation were carried out with a "Brilliant" Q-switched Nd-YAG laser delivering linearly polarized infrared radiation at $\lambda_1 =$ 1064 nm wavelength, $\tau_p = 4.5$ ns pulse duration at 10 Hz repetition rate, and D=6 mm beam diameter measured at $\frac{1}{e^2}$ of the Gaussian intensity profile. Laser pulses were focused on open air at ambient pressure P=760 Torr, by a f=3 cm focal-length lens, giving beam radius in focus $w_0 \cong 3.4$ μ m and a peak intensity I_0 in the range of 10 to 140 TW cm^{-2}. These intensities are above air breakdown threshold, in accordance to previously reported threshold power $P_{bt} = 1$ MW.

The harmonics radiation emerging from the breakdown plasma is analyzed in the axial direction with a fiber-coupled spectrometer (Ocean Optics HR2000+, 0.1 nm spectral resolution) triggered by the Q-switch signal of the laser system. The collecting fiber-tip was set in axial position ~ 8 cm away from the lens focus. The dependence of TH radiation on F intensity is given in Fig. 4(a). To characterize the directionality of TH emission, we measured the TH beam diameter at ~8 cm away from the lens focus, as follows: we mounted the collecting fiber-tip of the spectrometer on a 1D mechanical translation-stage of 10 μ m resolution and scanned it in transverse direction across the TH beam. The dependence of TH intensity on the position of the fiber-tip is presented in Fig. 4(b), revealing an approximate Gaussian profile of ~8 mm diameter, while F beam diameter at this position is 16 mm.

The influence of F polarization on the efficiency of THG was investigated by rotating a quarter waveplate in the range -45 to 45 degrees, with 5 degrees increment, to change the polarization state from circular to linear and back to circular (Fig. 4(c)). During plate rotation, the ellipticity ϵ was varied between -1 and 1, where $\epsilon = \pm 1$ correspond to circular polarization and $\epsilon = 0$ to linear polarization.

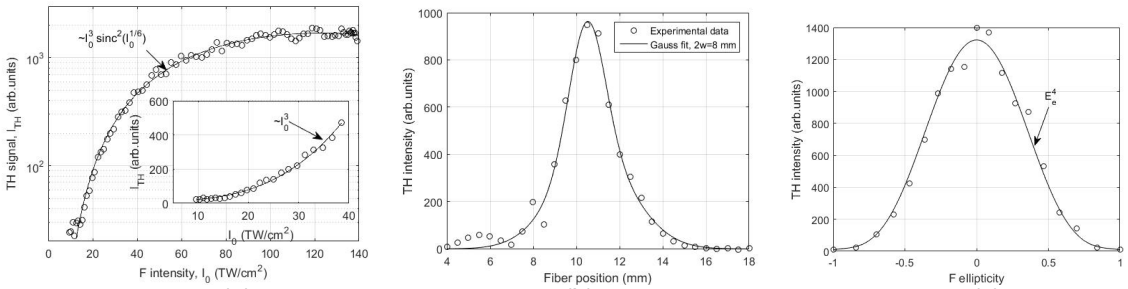

Fig. 4. (a) Experimental TH signal vs. F intensity. (b) TH signal recorded by translating radially the fiber-tip of the spectrometer. (c) TH signal vs. F ellipticity, . The solid line presents the fitting curve.

3. Deliverables in the last year related to the project:

- List of papers (journal or conference proceeding);

1 paper published: M. Stafe, “Three-step model for third-harmonic generation in air by nanosecond lasers”, JOURNAL OF THE OPTICAL SOCIETY OF AMERICA B-OPTICAL PHYSICS38 (7), 2206-2214 (2021)

- List of talks of group members (title, conference or meeting, date);

- Other deliverables (patents, books etc.).

- phase report.

4. Further group activities (max. 1 page):

- Collaborations, education, outreach.

M. Stafe, N. N. Puşcaş,and C. Negutu collaborate with INFLPR for studying theoretically and experimentally the target and particle acceleration by ultrashort high intensity laser pulses. They will publish their results in ISI journals.

Mihai Stafe, Niculae N. Puşcaş, Georgiana Vasile and Constantin Negutu collaborate with INOE for the project: ”Memorie inovativă optică plasmonică rapidă pe bază de anizotropie foto-indusă (FOMAN)”; 2020-2022, University POLITEHNICA of Bucharest being a partner of the project.

The knowledge acquired during this project is used for teaching two courses in the IALA master program at University Politehnica of Bucharest: 'Laser and Optics' given by Prof. Dr. Niculae.N. Puscas, and 'High Power Lasers Engineering and applications' given by S.I. Conf. Dr. Mihai Stafe.

Stage III. Experimental study on properties of harmonics and their influence on characteristics of comercial optical fibres used near the target

Activity A III.1. Experimental study on properties of harmonics in relation to properties of driving laser in focus for laser diagnosis.

We will analyse the influence of the irradiation parameters on the properties of the harmonics radiation in order to establish a diagnosing method for the driving laser intensity in focus from the harmonics spectrum. We will use spectrometer in the UV-VIS domain: 200-600 nm fibre-coupled “Ocean Optics” spectrometer with 0.2 ns resolution (available at

LILS) for low harmonics, and ~50-200 nmfor high order harmonics (to be acquired). Also, rapid photodiode (available at LILS) and single-pulse auto-correlator (from “Light Conversion”, available at LILS) will be used in order to analyse the nanosecond-femtosecond signals.

Activity A III.2. Determination of main characteristics of optical fibres used near the target when exposed to UV, X and gamma radiation.

We will investigate the modification of the fibre properties after irradiation with UV, X and gamma radiation:near-field measurements of optical fibres, investigations of the radiation-induced attenuation, microscopic study regarding structural and compositional characterization of the fiber material (before and after irradiation).

Activity A III.3. Project management anddisemination of results.

We propose to present the results in 1 ISI scientific paper and at 1 conference.